Stopping single photons in one-dimensional circuit quantum electrodynamics systems

Jung-Tsung Shen, M. L. Povinelli, Sunil Sandhu, and Shanhui Fan*
Ginzton Laboratory, Stanford University, Stanford, California 94305, USA
(Received 9 June 2006; revised manuscript received 16 November 2006; published 12 January 2007)

We propose a mechanism to stop and time reverse single photons in one-dimensional circuit quantum electrodynamics systems. As a concrete example, we exploit the large tunability of the superconducting charge quantum bit (charge qubit) to predict one-photon transport properties in multiple-qubit systems with dynamically controlled transition frequencies. In particular, two qubits coupled to a waveguide give rise to a single-photon transmission line shape that is analogous to electromagnetically induced transparency in atomic systems. Furthermore, by cascading double-qubit structures to form an array and dynamically controlling the qubit transition frequencies, a single photon can be stopped, stored, and time reversed. With a properly designed array, two photons can be stopped and stored in the system at the same time. Moreover, the unit cell of the array can be designed to be of deep subwavelength scale, miniaturizing the circuit.

DOI: 10.1103/PhysRevB.75.035320 PACS number(s): 74.50.+r, 32.80.−t, 03.67.Lx, 42.50.−p

Single photon transport properties in circuit quantum electrodynamics (circuit QED) systems are expected to play a significant role in quantum information processing and quantum computing. In contrast to cavity QED, where a single photon is confined in a cavity with a discrete photonic mode spectrum, in a circuit QED system, the single photon propagates in a one-dimensional continuum. In a recent solid-state experimental implementation of circuit QED, a single photon on average is coupled to a superconducting charge quantum bit (charge qubit), or Cooper pair box, in a one-dimensional coplanar waveguide geometry. Strong coupling between the single photon and the qubit has been demonstrated.[1] Theoretically, it was also shown that the one-dimensional propagating continuum of the single photon leads to versatile transmission and reflection profiles, including general Fano line shapes, and allows one-photon switching.[2,3] The proposed formalism in Refs. 2 and 3 is very general and encompasses the experiment in Ref. 1 as a special case.

The Cooper pair box is highly tunable, as compared to other qubit implementations, such as hyperfine structure in real atoms, quantum dots, or optical resonators. The transition energy of the Cooper pair box can easily be tuned by threading the Josephson junction loop with a magnetic field flux.[1,4–8] In this paper, we exploit the large tunability of the qubit to predict one-photon transport properties in multiple-qubit systems with dynamically controlled transition frequencies. In particular, two qubits coupled to a waveguide give rise to a single-photon transmission line shape that is analogous to electromagnetically induced transparency (EIT) in atomic systems. The width of the transparency peak is strongly tunable by adjusting the transition frequencies. Furthermore, by cascading double-qubit structures to form an array, the properties of photons inside the array are now determined by a photonic band structure. By dynamically tuning the transition frequency of the qubits while the photon is in the array, the band structure and the spectrum of the single photon can be molded almost arbitrarily, leading to highly nontrivial information processing capabilities on chip, including stopping, storing, and time reversal of a single-photon pulse. Moreover, with a properly designed array, two photons can be stopped and stored in the system at the same time. Finally, the unit cell of the array can be designed to be of deep subwavelength scale, miniaturizing the circuit. Possible applications of single-photon manipulation schemes demonstrated here include logic gates, memory, buffers, and repeaters in quantum information processing and quantum communication.

To start with, consider the simplest case of one qubit coupled to a waveguide. In Refs. 2 and 3, it was shown that the transfer matrix T_q of a single photon[9] passing through a single qubit takes the following form:

$$\begin{pmatrix} a' \\ b' \end{pmatrix} = \begin{pmatrix} 1 - \dfrac{iV^2}{v_g(\omega_k - \Omega + i\gamma)} & -\dfrac{iV^2}{v_g(\omega_k - \Omega + i\gamma)} \\ +\dfrac{iV^2}{v_g(\omega_k - \Omega + i\gamma)} & 1 + \dfrac{iV^2}{v_g(\omega_k - \Omega + i\gamma)} \end{pmatrix} \begin{pmatrix} a \\ b \end{pmatrix} \equiv T_q(\Omega) \begin{pmatrix} a \\ b \end{pmatrix}, \quad (1)$$

where Ω is the transition frequency of the qubit, $\omega_k = v_g k$ is the frequency of the photon, v_g is the group velocity of the fundamental waveguide mode, and V is the coupling constant between the photons and the qubits. γ accounts for loss mechanisms. To highlight the intrinsic behavior of the system, we set γ equal to zero. Discussion of the effects of a nonzero γ is provided at the end of the paper. The transfer matrix relates the incoming and outgoing wave amplitudes $a(b')$ and $b(a')$ on either side of the qubit. Note the form of the transfer matrix is the same as for a waveguide side coupled to a single-mode optical cavity.[10–12] The exact mapping implies that the one-photon system in discussion exhibits many features that have been well studied for cavity structures and classical light. The mapping is quite interesting given that the microscopic theories that underlie these systems are very different.

The transfer matrix T_q [Eq. (1)] allows the complete determination of photon transport properties. The response function of any configuration of mutiple qubits can be calculated by cascading the transfer matrices of each individual element in the system. For example, the total transfer matrix

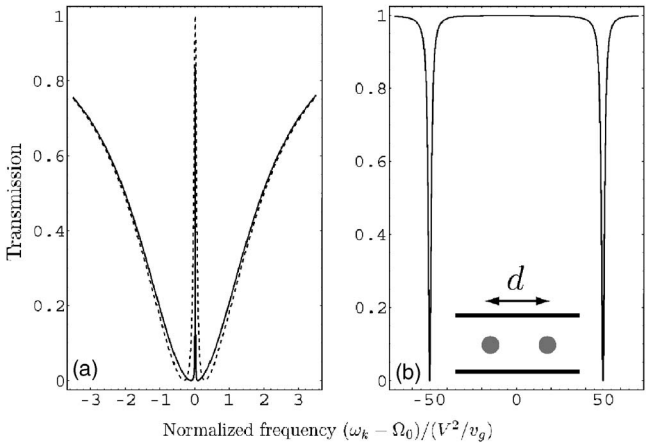

FIG. 1. Transmission spectrum of two closely spaced ($d \ll \lambda$) qubits coupled to a waveguide. A schematic of the two qubits in the waveguide is shown. The qubits have transition frequencies Ω_1 and Ω_2, respectively. $\Omega_0 \equiv (\Omega_1+\Omega_2)/2$. The normalized detuning $\Delta \equiv |\Omega_1-\Omega_2|/(V^2/v_g)$. (a) Small detuning regime. Solid curve: $\Delta=0.2$; dashed curve: $\Delta=0.6$. (b) Large detuning regime. $\Delta=100$. The transmission spectrum is obtained from Eq. (1). $\phi(d)$ is taken as 10^{-2} in both figures. The two minima in each transmission spectrum are at Ω_1 and Ω_2, respectively.

for a system consisting of two qubits with transition frequencies Ω_1 and Ω_2, respectively, separated by a distance d is[13]

$$T \equiv T_q(\Omega_1)\begin{pmatrix} e^{i\phi(d)} & 0 \\ 0 & e^{-i\phi(d)} \end{pmatrix} T_q(\Omega_2) \equiv T_q(\Omega_1)T_p(d)T_q(\Omega_2), \tag{2}$$

where $T_p(d)$ is the propagation matrix, and $\phi(d)=\omega_k/v_g d$ is the phase accumulation as the photon travels through the distance d.

In general, the transmission spectrum of a two-qubit system strongly depends on the ratio of coupling strength to the difference between qubit frequencies, as well as the separation distance. Since in practice it is of interest to miniaturize the circuits, we focus upon the regime where the separation distance d is much less than the wavelength λ in the waveguide, $d \ll \lambda$. When $\Omega_1 \neq \Omega_2$, a transparency peak with 100% transmission emerges in the transmission spectrum. In the small detuning regime ($|\Omega_1-\Omega_2| \ll V^2/v_g$), the transparency peak is very narrow, as shown in Fig. 1(a). The two minima in the transmission spectrum are at Ω_1 and Ω_2, respectively, and each of which reflects the minimum of the transmission spectrum for the case of the single photons interacting with a single qubit.[2,3] Moreover, the peak width is easily adjustable via tuning of the qubit transition frequencies. The appearance of the peak is analogous to the EIT phenomenon in atomic vapor systems.[14–17] We note that EIT-like interference has previously been investigated in a flux (current-biased) qubit system.[18] Our work, however, explicitly calculates single-photon transport properties. Furthermore, in the conventional EIT phenomena based on three-level systems, both the "control" laser as well as the "probe" laser are present to correlate the three levels. In contrast, in the above two-qubit system, the condition of the single photon imposes a constraint that correlates the two qubits, and there is no control beam. Both systems give the same transmission line shape. In the large detuning regime ($V^2/v_g \ll |\Omega_1-\Omega_2|$), the transmission spectrum features a very broad plateau, as shown in Fig. 1(b), with a full width approximately equal to $|\Omega_1-\Omega_2|/(V^2/v_g)$. In this large detuning regime, the two qubits are essentially decoupled. The transmission spectrum is thus a simple combination of that of each qubit.[2,3] By tuning the transition frequencies of the qubits, one can switch the system between these two regimes.

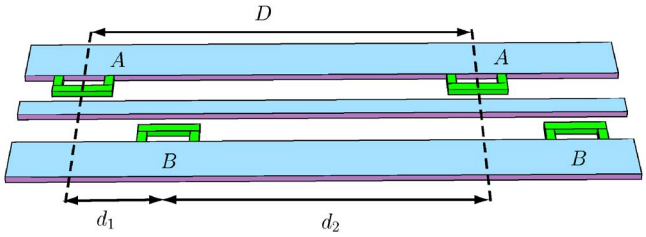

FIG. 2. (Color online) Schematic of a tunable one-dimensional qubit-waveguide system used to stop and store a single photon. The system consists of a periodic array of unit cells of length D. Each unit cell consists of two qubits, A and B, separated by a distance d_1. The three horizontal bars represent the one-dimensional transmission line waveguide.

Unit cells of two qubits can be arranged in a periodic array, as shown in Fig. 2. The transparency peaks corresponding to single unit cell couple to form a band. The photonic band structure can be designed by choosing the appropriate distances between the qubits, and can be further dynamically tuned by adjusting the qubit resonant frequencies. Dynamic tuning of photonic band structures has previously been studied in classical optical resonator systems.[19–23] By choosing an initial photonic band structure that has a large bandwidth to allow a photon to enter the system, and by compressing the width of the photonic band adiabatically while maintaining translational symmetry, a classical pulse can be slowed down, or even stopped and stored in the system.[19–23] Moreover, when the conditions are satisfied such that the sign of the slope of the band is flipped, the wave packet of the pulse can be time reversed. Here, we show that circuit QED provides the capability for single-photon stopping, storing, and time reversal. Distinct from implementations in classical optical resonator systems, in the superconducting qubit systems, the size of the individual qubits as well as the unit cell can be far smaller than the wavelength. Also, the resonant frequencies of the qubits are several order of magnitudes more tunable compared with other systems. These properties provide potential for stopping-light experiments. As a concrete example, we apply these principles to a one-dimensional circuit QED systems consisting of a periodic array of superconducting charge qubits to stop and time reverse single photons in the microwave frequency range.

Below, we highlight some of the consequences of these properties by focusing on two schemes characterized by how the qubit frequencies vary during the dynamic process: (ii) Detuning Δ is varying. In this scheme, a light pulse is stopped by reducing Δ, similar to Ref. 20. The interesting feature is that the size of the unit cell can be designed to be

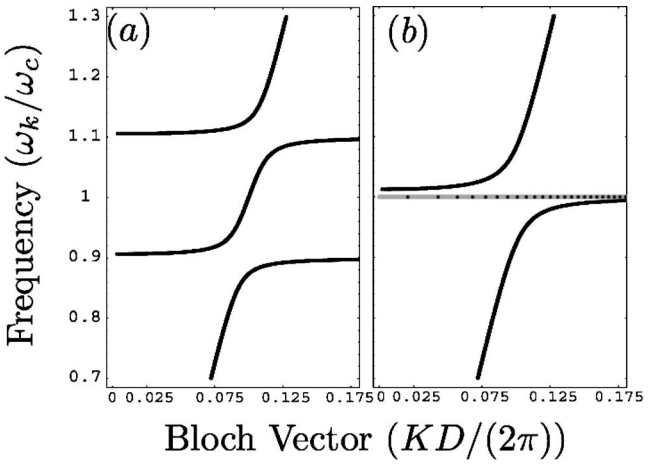

FIG. 3. The photonic bands of the system related to tuning scheme (i). The qubits frequencies are given by $\Omega_{A,B}=\omega_c\pm(1/2)\Delta(V^2/v_g)$. $V^2/v_g=2\times10^{-4}\omega_0$. $\omega_0\equiv2\pi v_g/D$. $d_1=0.3D$ in all cases. (a) Large detuning regime. $\Delta=100$. $\omega_c\equiv0.1\omega_0$. (b) Small detuning regime. $\Delta=0.6$. $\omega_c\equiv0.1\omega_0$.

of deep subwavelength, while in previous optical resonator implementations, the unit cell sizes are necessarily comparable to the wavelength. (ii) Δ is fixed. In this scheme, a light pulse is stopped as well as time reversed by changing the resonant frequencies of all qubits simultaneously, all with a unit cell size that is approximately half the wavelength.

We first examine the dispersion relation as a function of the qubit frequencies. The dispersion relation between the eigenstate frequency ω and the Bloch wave vector K of the periodic system can be obtained from the transfer matrix of the unit cell $T_{\text{cell}}\equiv T_q(\Omega_1)T_p(d_1)T_q(\Omega_2)T_p(d_2)$ by[20]

$$\cos[K(\Omega_1,\Omega_2,d_1,\omega_k)D] = \frac{1}{2}\,\text{Trace}(T_{\text{cell}}) = \cos[(\omega_k/v_g)D] + \frac{C_+}{\omega_k-\Omega_1} + \frac{C_-}{\omega_k-\Omega_2}, \tag{3}$$

where[24]

$$C_\pm = \sin[(\omega_k/v_g)D](V^2/v_g) \pm 2\sin[(\omega_k/v_g)d_1]\sin[(\omega_k/v_g)d_2] \times (V^2/v_g)^2\frac{1}{\Omega_1-\Omega_2}, \tag{4}$$

where D is the length of the unit cell, d_1 is the distance between the two qubits in the unit cell, and $d_2\equiv D-d_1$. Using these equations, we now discuss the two schemes indicated earlier.

Scheme (i): Detuning Δ *is dynamically reduced*. The band diagram of the periodic system strongly depends on Δ. Figure 3(a) shows the band diagram in the large detuning regime [$\Delta=100$, corresponding to Fig. 1(b)], where the middle band has a very large bandwidth. The bandwidth is proportional to the detuning Δ. Figure 3(b) shows the band diagram in the small detuning regime [$\Delta=0.6$, corresponding to Fig. 1(a)]. The width of the middle band is compressed to essentially zero; the group velocity is thereby vanishingly small. The value of Δ at which the slope of the middle band is exactly zero can be obtained from Eqs. (3) and (4).[20] Tuning Δ to change the band structure from Figs. 3(a) and 3(b), while a pulse is in the system, allows the stopping of a pulse.[20] For Fig. 3(a), the middle band is centered at frequency $\omega_c\equiv0.1(2\pi v_g/D)=1/2(\Omega_A+\Omega_B)$, which corresponds to a unit cell size $D=\lambda/10$, i.e., the unit cell is of deep subwavelength. In this scheme, provided that there is no direct couplings between qubits in different unit cells, one can further miniaturize the size of the unit cell.

To achieve time reversal, it is necessary to have a unit cell size comparable to half the wavelength. Time reversal requires reversing the slope of a band. A simple criterion for the existence of negative slope can be obtained by taking the derivative of the dispersion relation [Eq. (3)]:

$$\frac{d\bar{\omega}}{d\bar{K}}\left(\frac{4}{\Delta^2}+1\right)2\pi\sin(2\pi\bar{\omega}) = 2\pi\sin(2\pi\bar{K}) + \frac{4}{\Delta^2}2\pi(1-2\bar{d}_1)\sin[2\pi\bar{\omega}(1-2\bar{d}_1)], \tag{5}$$

where the barred symbols are normalized dimensionless quantities defined as $\bar{\omega}\equiv\omega_k/\omega_0=D/\lambda$, $\bar{K}\equiv K/k_0$, and $\bar{d_1}\equiv d_1/D$; where $\omega_0\equiv2\pi v_g/D$, and $k_0\equiv2\pi/D$ are the frequency and wave vector unit, respectively. By symmetry we only need to investigate the range $\bar{d_1}<1/2$. In addition, $\bar{K}\leqslant1/2$ in the restricted first Brillouin zone. In the large detuning regime ($\Delta\gg1$), by requiring $d\bar{\omega}/d\bar{K}<0$, we obtain a simple relation

$$\frac{1}{2}<\bar{\omega}=D/\lambda. \tag{6}$$

With a large unit cell, one can achieve both stopping and time reversal by varying the detuning alone.[19–23]

Scheme (ii): Δ *is kept fixed, and* ω_c *is modulated*. When ω_c is larger than $0.5(2\pi v_g/D)$, the middle band shows a negative slope centered at ω_c and Bloch vector k_c [Fig. 4(a)]. As ω_c is gradually reduced, the bandwidth is dynamically compressed to zero [Fig. 4(b)]. As ω_c is further reduced, the slope is flipped and becomes positive hereafter, accomplishing a time reversal process [Figs. 4(c) and 4(d)].

Interestingly, in this scheme we can stop two single photons of different frequencies in the quantum circuit at the same time, since there are actually two flat bands in the system [Fig. 4(b)]. Assume that the system has gone through the dynamic process from Fig. 4(a) to Fig. 4(c) and a photon is stopped in the phase space indicated by the open circle. Notice that at this stage, an additional band is available at a lower frequency with a finite slope to accommodate the second incident photon, as indicated by the solid circle. After the second photon enters the system, the system is brought back to the stage denoted by Fig. 4(b), where both bands are flat, and thereby two photons are being held indefinitely in the system in two separate bands. To release either photon, one can bring the system to the stage of either Figs. 4(a) and 4(d), where either photon can be released. These two photons

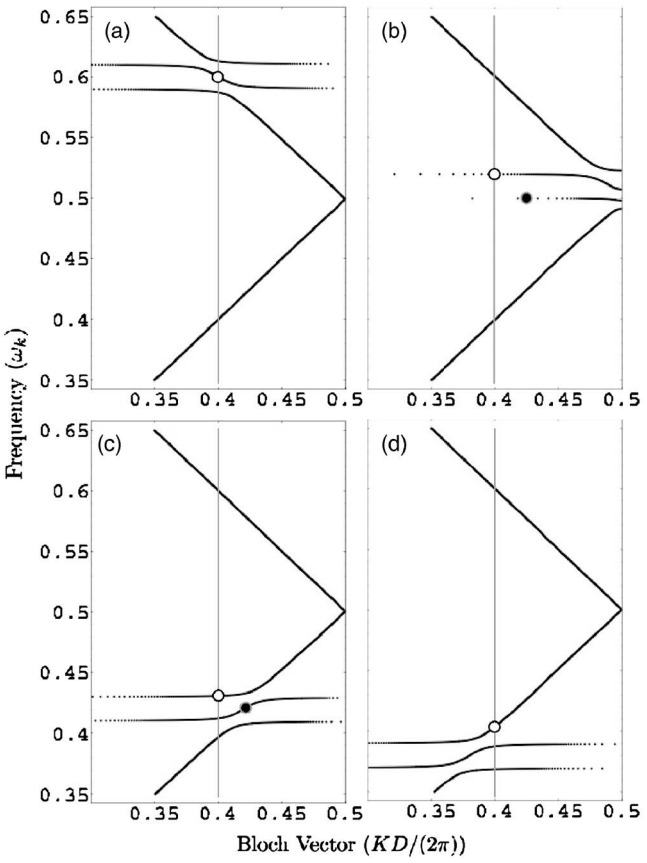

FIG. 4. The photonic bands of the system related to tuning scheme (ii). The circles denote the photon states in phase space. k_c for the open circle is chosen as $0.4[KD/(2\pi)]$ and is indicated by the vertical line. $\Delta \equiv |\Omega_1 - \Omega_2|/(V^2/v_g) = 100$. $\omega_0 \equiv 2\pi v_g/D$. $d_1 = 0.3D$. $V^2/v_g = 2\times 10^{-4}\omega_0$. (a) $\omega_c = 0.6\omega_0$. (b) $\omega_c = 0.51\omega_0$. (c) $\omega_c = 0.42\omega_0$. (d) $\omega_c = 0.38\omega_0$.

might need to be spatially separated to avoid interferences at the qubits so the stopping scheme would work, since the picture of band structure relies on the single-photon transfer matrix T_q [Eq. (1)].

To measure single-photon transmission spectra like those shown in Fig. 1, one would ideally use an input source of single photons generated on demand. In practice, experiments have shown[1] that single-photon transport can also be probed in constant-frequency, steady-state classical heterodyne measurements by attenuating the power of a multiphoton source to subphoton levels. To further observe the slowing and stopping of single photons, time-resolved measurements can be made. In the dynamical light-stopping scheme, the delay is controlled largely by the tuning time. By recording the delay in arrival time at a detector relative to a reference pulse that does not interact with the qubit system, slowing effects can be probed directly. Recently, a quantum scheme that allows for deterministic generation and homodyne detection of microwave photons in Fock states has been proposed.[25]

To implement the scheme discussed here, ideally one would like the qubit-waveguide coupling rate V^2/v_g to dominate the intrinsic loss rate of the qubit γ, which results from the qubit coupling to the environment external to the waveguide. At present, in the experiment reported in Ref. 1, V^2/v_g is inferred to be of the order of $2\pi\times 10^{-2}$ MHz, and γ is about $2\pi\times 0.7$ MHz. However, one could enhance V^2/v_g by reducing the group velocity in the waveguide, which could be accomplished, for example, with the use of coupled resonator waveguide structures;[26] or by increasing the dipole moment by using a larger qubit. Also, it has been emphasized that the current experimental value of γ of the state-of-the-art charge qubits is probably due to dielectric loss in the junctions or the substrate.[27] An improvement in the fabrication process and in the materials used could significantly improve them. The storage time is limited to $1/\gamma$. As an example, we consider stopping a single-photon pulse with a bandwidth of 1 GHz and a center frequency of 6 GHz. The superconducting qubits have a large tunable frequency range from approximately 0 to 8 GHz,[1] which is far more than enough to compress a 1 GHz bandwidth to zero. The minimum size of the circuit L is approximately $v_{g0}/f + l_0$, where v_{g0} is the initial group velocity of the photon, f is the modulation rate of the qubit frequency, and $l_0 \equiv v_{g0}\tau_{\text{pulse}}$ is the size of the pulse in the waveguide.[22] $v_{g0}\tau_{\text{pulse}}$ is roughly a constant independent of the pulse bandwidth $\Delta\omega$, and can be estimated as $10D$ for the dispersion relation.[22] The length of the waveguide is thus approximately $L \simeq (\Delta\omega/f + 10)D$. To accomplish the entire process of stopping and recovering a 1 ns pulse (i.e., bandwidth 1 GHz), a waveguide with length less than 17 unit cells modulated at a speed of 1 GHz is sufficient. This amounts to 1.7 carrier wavelength when the size of the unit cell is one-tenth of the wavelength. To modulate the magnetic field, one of the possible implementations is to use planar micron-scale metal coils. This technique has been adopted in atom manipulation, as well as electron spin resonance experiments,[28,29] and has been demonstrated to operate at GHz frequency range.[29]

The authors gratefully acknowledge the informative and helpful discussions with David Goldhaber-Gordon at Stanford Univeristy, Cheng Chin at the University of Chicago, Steven Girvin at Yale University, Travis Hime, and Hsiao-Mei (Sherry) Cho at UC Berkeley. Shanhui Fan acknowledges helpful discussions with M. F. Yanik and financial support by NSF Grant No. ECS-0134607, AFOSR Grant No. FA9550-05-1-0414, and the Packard Foundation.

*Electronic address: shanhui@standford.edu

[1] A. Wallraff, D. I. Schuster, A. Blais, L. Frunzio, R.-S. Huang, J. Majer, S. Kumar, S. M. Girvin, and R. J. Schoelkopf, Nature (London) **431**, 162 (2004).
[2] J. T. Shen and S. Fan, Opt. Lett. **30**, 2001 (2005).
[3] J.-T. Shen and S. Fan, Phys. Rev. Lett. **95**, 213001 (2005).
[4] V. Bouchiat, D. Vion, P. Joyez, D. Esteve, and M. H. Devoret, Phys. Scr. **T76**, 165 (1998).
[5] Y. Nakamura, Y. A. Pashkin, and J. S. Tsai, Nature (London) **398**, 786 (1999).
[6] D. Vion, A. Aassime, A. Cottet, P. Joyez, H. Pothier, C. Urbina, E. Esteve, and M. H. Devoret, Science **296**, 886 (2002).
[7] Y. Makhlin, G. Schön, and A. Shnirman, Rev. Mod. Phys. **73**, 357 (2001).
[8] M. H. Devoret, A. Wallraff, and J. M. Martinis, cond-mat/0411174 (unpublished).
[9] Here the single photon refers to a photon in Fock state, labeled by the wave vector k. These Fock states form a complete set and could be used as basis to expand a single-photon wave packet.
[10] H. A. Haus and Y. Lai, J. Lightwave Technol. **9**, 754 (1991).
[11] Y. Xu, Y. Li, R. K. Lee, and A. Yariv, Phys. Rev. E **62**, 7389 (2000).
[12] S. Fan, Appl. Phys. Lett. **80**, 908 (2002).
[13] P. Yeh, *Optical Waves in Layered Media* (John Wiley & Sons, New York, 1988).
[14] S. E. Harris, Phys. Today **50** (7), 36 (1997).
[15] L. V. Hau, S. E. Harris, Z. Dutton, and C. H. Behroozi, Nature (London) **397**, 594 (1999).
[16] M. D. Lukin and A. Imamoglu, Nature (London) **413**, 273 (2001).
[17] J. P. Marangos, J. Mod. Opt. **45**, 471 (1998).
[18] K. V. R. M. Murali, Z. Dutton, W. D. Oliver, D. S. Crankshaw, and T. P. Orlando, Phys. Rev. Lett. **93**, 087003 (2004).
[19] M. F. Yanik and S. Fan, Phys. Rev. Lett. **92**, 083901 (2004).
[20] M. F. Yanik, W. Suh, Z. Wang, and S. Fan, Phys. Rev. Lett. **93**, 233903 (2004).
[21] M. F. Yanik and S. Fan, Phys. Rev. Lett. **93**, 173903 (2004).
[22] M. F. Yanik and S. Fan, Phys. Rev. A **71**, 013803 (2005).
[23] M. F. Yanik and S. Fan, Stud. Appl. Math. **115**, 233 (2005).
[24] We have corrected a sign error in Ref. 20.
[25] M. Mariantoni, M. J. Storcz, F. K. Wilhelm, W. D. Oliver, A. Emmert, A. Marx, R. Gross, H. Christ, and E. Solano, cond-mat/0509737 (unpublished).
[26] A. Yariv, Y. Xu, R. K. Lee, and A. Scherer, Opt. Lett. **24**, 711 (1999).
[27] J. M. Martinis, K. B. Cooper, R. McDermott, M. Steffen, M. Ansmann, K. D. Osborn, K. Cicak, S. Oh, D. P. Pappas, R. W. Simmonds *et al.*, Phys. Rev. Lett. **95**, 210503 (2005).
[28] M. Drndic, K. S. Johnson, J. H. Thywissen, M. Prentiss, and R. M. Westervelt, Appl. Phys. Lett. **72**, 2906 (1998).
[29] G. Boero, M. Bouterfas, C. Massin, F. Vincent, P.-A. Besse, R. S. Popovic, and A. Schweiger, Rev. Sci. Instrum. **74**, 4794 (2003).